

# Symmetry and substrate effects on magnetic interactions from first principles: A comparison between Fe/W(100) and Fe/W(110)

X. Qian<sup>1</sup> and W. Hübner<sup>2</sup><sup>1</sup>*Department of Physics, Colorado State University, Fort Collins, Colorado 80523*<sup>2</sup>*Max-Planck-Institut für Mikrostrukturphysik, Weinberg 2, D-06120, Halle, Germany*

(Received 16 September 2002; revised manuscript received 16 December 2002; published 22 May 2003)

The *ab initio* full-potential linearized augmented plane-wave (FP-LAPW) method was employed to investigate the magnetic properties of 1 monolayer (ML) Fe on W(100) and W(110) substrates. Theoretical study reveals very different characteristics arising from the Fe-Fe and Fe-W interactions in these two systems, which include Fe-W relaxations, magnetic moments, and interlayer exchange couplings. The origin of these differences is considered by the crystal-field effects in these two crystallographic orientations. We show that symmetry plays a crucial role in the Fe-Fe and Fe-W interlayer interactions in Fe/W ultrathin magnetic films.

DOI: 10.1103/PhysRevB.67.184414

PACS number(s): 75.70.Ak, 75.70.Cn, 71.70.Ch, 68.43.Bc

## I. INTRODUCTION

Ultrathin Fe films grown on W(100) and W(110) substrates are prototype magnetic systems for studying thin-film magnetism<sup>1–24</sup> due to their thermal stability, large lattice mismatch of 9.4%, and pseudomorphic growth. Fe films deposited on W(100) and W(110) substrates exhibit very different magnetic properties.<sup>3,8,12,16,21</sup> While submonolayer Fe on W(110) is magnetic,<sup>2–4,8,12,19,22</sup> no magnetic signal has been observed on W(100) substrate.<sup>6,7,21</sup> So far, this difference has not been extensively explored nor understood. Here we attempt to illustrate the differences between the two systems with their atomic symmetries and their subsequent effect on the overlayer-substrate interactions for the (100) and (110) crystal orientations. The crystallographic orientation dependence of magnetism has also been observed for the interlayer exchange coupling in multilayer magnetic systems.<sup>25</sup>

Exchange coupling between atomic layers constitutes many interesting phenomena including giant magnetoresistance (GMR) and spin waves in magnetic multilayer. Two theories have been developed and employed to explain the interlayer exchange couplings.<sup>26,27</sup> One is based on the Ruderman-Kittel-Kasuya-Yosida (RKKY) spin-dependent scattering model.<sup>26</sup> The other is based on the quantum size effect, i.e., the modulation of density of states (DOS) due to quantum confinement.<sup>27</sup> These two theories are quite successful in explaining most of the experimental observations.<sup>28</sup> Despite the good agreement in GMR between theory and experiment, there is one aspect that deserves further attention. So far the short oscillation periods of the exchange coupling predicted by theory in the (110) oriented multilayer have not been observed in experiments.<sup>28</sup> Some ascribe such a discrepancy to the surface and interface roughness or disorder effect.<sup>29,30</sup> Indeed, including disorder in the calculations, the short oscillation periods could disappear.<sup>29</sup> However, the underlying mechanism is still quite controversial. Understanding exchange coupling on the short-range scale is necessary in order to understand the effects of interface atomic structure on GMR.

In addition to interlayer exchange coupling, the origin of ferromagnetism in metals is still not completely

understood.<sup>31–33</sup> The role that intra-atomic and interatomic exchange interaction plays in ferromagnetism is still not clear. Whether these two interactions are collaborative or competing largely depends on the system and its atomic structure under study. Generally speaking, larger interatomic distance favors ferromagnetism for interatomic exchange interaction dominated systems and leads to an enhanced magnetic moment. At a given interatomic spacing, whether the system is ferromagnetic or not will depend on many competing interactions including magnetic, electronic, elastic, and magnetoelastic interactions that eventually lead to the lowest energy state. The situation is more complicated when there is an interface (e.g., Fe/W), where the hybridization or interaction between the two interfacial elements will be added. It is particularly subtle when magnetism is dominated by the interatomic exchange interaction because of its sensitivity to chemical bonding. However, the interface will also affect intra-atomic interaction due to the change in crystal field and therefore the width and splitting of the *d* band.

As is well known, magnetic moment is closely related to the nearest neighbor coordination number, the interatomic bond length, and the nature of chemical bonding between the atoms. According to the Stoner model,<sup>34</sup> ultimately it is the electronic structure including both the majority and minority spin bands that governs the appearance of magnetism according to the energy gain through exchange splitting. Since electronic structure is very sensitive to the symmetry and bond length of the atomic geometry, it is of great pertinence to study the geometric effect on magnetism. Since Fe, Co, and Ni are considered to be itinerant magnetic metals, the overall band structures and Fermi surfaces of these materials were studied earlier. For ultrathin magnetic films with no more than a few monolayer (ML) coverage on nonmagnetic substrate, it is the *3d* band of the magnetic element that determines the magnitude of the magnetic moment and its relative orientation. However, for the magnetic adsorbate, the effect of substrate on its electronic structure is significant. As a result, the crystal-field effect of the nearest neighbors will play a significant role on the splitting, degeneracy, and the relative positions of the five *d* ( $d_{xy}, d_{xz}, d_{yz}, d_{x^2-y^2}, d_{z^2}$ ) orbitals of the magnetic adsorbate atom. Even though crystal-field theory (or ligand-field theory) is mainly applied to metal

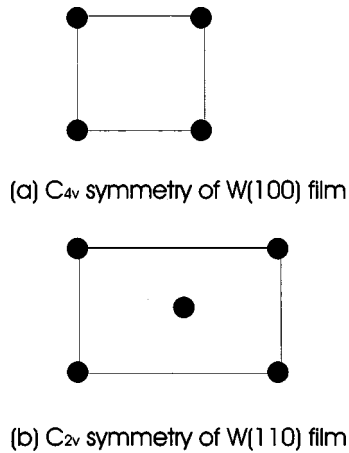


FIG. 1. Schematics of the  $C_{4v}$  and  $C_{2v}$  point-group symmetries for the two bcc crystal orientations (100) and (110).

oxides and to other ionic crystals, it is still valid and useful to consider the  $d$ -band splitting in metallic ultrathin films deposited on substrates since both interatomic and intra-atomic interaction will probably play an important role in these films. Actually crystal-field splitting is very similar to the on-site Coulomb repulsion  $U$  generally adopted in solid-state theory. The limitation of crystal-field theory is that only short-range nearest-neighbor interactions are considered. Nevertheless, it is still rather helpful in understanding the geometric effect on the magnetic moment and on the short-range interlayer exchange coupling.

## II. THE SYSTEMS

The Fe/W (110) and Fe/W (100) ultrathin films are prototype magnetic systems for providing insightful information on thin film magnetism. Comparison of two different crystal orientations is also very useful for understanding the lack of experimental evidence on the short oscillation periods of GMR as a function of spacer layer thickness in (110) oriented multilayer. Furthermore as stated earlier, it was observed that there are magnetic dead layers in the submonolayer coverage of Fe on W(100),<sup>21</sup> while an enhancement of the surface magnetic moment was observed for the 1 ML Fe/W(110) system.<sup>8,19,22</sup> Since electronic structure directly reflects the atomic structure of the system, magnetism is very sensitive to the details of the atomic structure. The nearest-neighbor Fe-Fe bond length of pseudomorphic layer on W(110) is only 0.866 of that on W(100). However, the Fe-W interlayer distance for W(100) is shorter than the one for W(110) and the Fe atom has four nearest-neighbor W atoms compared to the two atoms for the case of W(110). Thus Fe and W layers have a stronger interaction in the (100) oriented film than in the (110) film. In addition, 1 ML Fe/W(100) has a  $C_{4v}$  point-group symmetry, while 1 ML Fe/W(110) has a lower  $C_{2v}$  symmetry as shown in Fig. 1. Since symmetry is crucial in crystal-field splitting of the  $d$  orbitals, it is not unexpected that Fe/W(110) and Fe/W(100) films exhibit different magnetic properties. Moreover, the Fe-W interfacial layers are characterized as having a strong interaction due to the highly reactive nature of the W atoms. The Fe-W binding

energy is about 4.1 eV/atom.<sup>8</sup> Consequently this system is particularly suitable for the study of interlayer exchange interactions on a short-range atomic level. Further the strong hybridization between the valence  $s$ ,  $p$  orbitals and the more localized  $d$  orbitals makes crystal-field theory applicable for the study of Fe/W systems. The dependence of magnetic properties such as magnetic moment and interlayer exchange coupling on crystallographic orientation will be pronounced in this system since magnetic interaction is largely localized due to the relative strong interaction between the overlayer Fe and substrate W atoms.

For the free-standing Fe(110) or Fe(100) thin films, the magnetic moment of Fe is approximately proportional to the nearest-neighbor bond length and inversely proportional to the coordination number since the density of states (DOS) is broader for shorter bond distance and larger coordination number. Consequently for shorter interatomic distance and large coordination number, the DOS at the Fermi level is reduced, hence a smaller magnetic moment is expected. Earlier calculations<sup>7</sup> and our present *ab initio* calculations show that Fe atoms have moments of around  $3.3\mu_B$  and  $2.9\mu_B$ , respectively, for the 1 ML free-standing Fe(100) and Fe(110) film with the same bcc Fe lattice parameter  $a$  of 2.86 Å. Both of these values are enhanced compared to  $2.2\mu_B$  for the bulk bcc Fe. The smaller moment in Fe(110) is due to the shorter nearest-neighbor distances in the (110) oriented film compared to that of (100) orientation. However, for 1 ML Fe/W(100) and 1 ML Fe/W(110), an opposite trend is observed. In both experiments<sup>3</sup> and theoretical calculations,<sup>19</sup> it was found that Fe has an enhanced moment of about  $2.56\mu_B$  in 1 ML Fe/W(110) film compared to the moment of  $2.2\mu_B$  in bulk bcc Fe. Further, a Curie temperature of 282 K was observed for the monolayer Fe on W(110).<sup>3,8</sup> These results are contrary to those of Fe free-standing films. According to the above mentioned argument, Fe atoms should possess a larger magnetic moment on a W(100) substrate if only the nearest-neighbor interactions are taken into account. Further, the submonolayer Fe films are grown pseudomorphically on both the W(100) and W(110) substrates.<sup>1,12,21</sup> Therefore the unexpected experimental result of vanishing magnetic moment for Fe on W(100) must be related to the interaction between Fe and W atoms. A major difference between the (110) and (100) oriented atomic structures is the symmetry, symmetry must play an important role in the interaction between the Fe overlayer and the W substrate. Indeed, according to crystal-field theory, the  $3d$  orbitals will be split into different bands for different symmetry. As a result, the interaction between Fe and W will be greatly affected by the symmetry. Consequently both the interlayer exchange interaction and magnetic moment will strongly depend on the crystal symmetry and orientation of the films.

For a heterogeneous epitaxial layer on a substrate, the crystal-field effect on the atom of an interfacial adsorbed layer comes from two sources, one is due to the neighboring atoms in the same adsorbed layer, and the other arises from the neighboring substrate atoms. Similar to the magnetic moment, the relative strength of the crystal field depends on the nature of chemical bonding and geometric effects. Figure 2 illustrates the  $d$ -orbital splitting due to the crystal-field effect

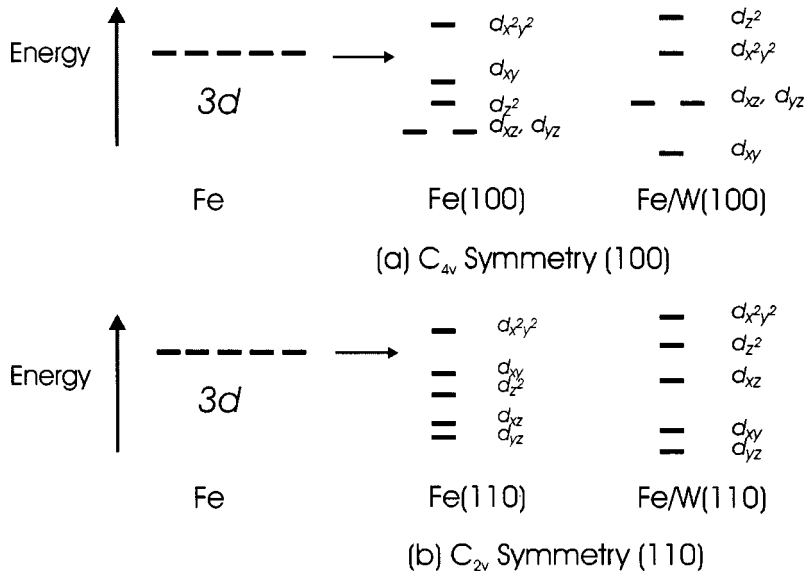


FIG. 2. Schematics of crystal-field splitting for the Fe atoms in  $C_{4v}$  and  $C_{2v}$  crystal symmetry environment at the  $\Gamma$  point.

in free-standing Fe monolayer films and with W substrates. According to crystal-field theory, the relative positions of the  $d$  orbitals are determined by their symmetries and the positions of the neighboring atoms. The width of crystal-field splitting could be measured by the width of the  $d$ -DOS. The overall width for the overlayer Fe  $3d$  orbitals is about 5 eV (Ref. 19) for 1 ML Fe on W(110). The crystal-field splitting for the W  $5d$  orbitals is about 10 eV.<sup>19</sup>

Crystal-field splitting affects not only magnetism (e.g., Hund's second rule), but also the relative orientations of the spin and orbital moments, i.e., Hund's third rule. Rigorously, Hund's second and third rules are only valid for isolated atoms. In a crystal environment, when crystal-field splitting is of the order of electron-electron exchange interaction, Hund's third rule may no longer hold. There are only a few cases where a violation of Hund's third rule was observed.<sup>19,22,35-37</sup> Violations are observed for the interfacial W atoms in Fe/W(100) from experiments<sup>37</sup> and in Fe/W(110) from earlier *ab initio* calculations.<sup>19,22</sup> The reason is perhaps due to the large crystal-field splitting of W  $5d$  orbitals since the W  $5d$  orbitals are affected strongly by the neighboring atoms. The  $5d$  density of states of W is broadened to be  $\sim 10$  eV which is twice as much as  $3d$  DOS broadening for Fe.

### III. RESULTS AND DISCUSSION

The WIEN97 code<sup>38</sup> based on FP-LAPW method was used to carry out the calculations. Repeated slab geometries consisting of a total of five W substrate layers and one Fe layer on each surface were employed in all of the calculations. A total of eight vacuum layers were used to separate the interactions between the slabs. The same number of  $k$  points of 3000 in the full Brillouin zone was used for both Fe/W(110) and Fe/W(100) films to ensure a proper comparison. The generalized gradient approximation (GGA) was adopted for the exchange-correlation functional. Spin-orbit coupling for the valence electrons was not included in the calculations. Additional computational details were described in our earlier publications.<sup>19,23</sup>

The theoretical bcc W lattice constant of 3.205 Å was used for the in-plane lattice parameter in 1 ML Fe/W(110) and 1 ML Fe/W(100) films. By comparing the results from the films with the same in-plane lattice parameter, the differences in structure and magnetism between these two systems could be attributed to the difference in symmetry and the subsequent Fe-Fe and Fe-W interactions. In addition, two more calculations at different lattice parameters of 3.165 and 3.123 Å were carried out for 1 ML Fe/W(100) in order to check the effect of lattice parameter change on structural and magnetic properties while keeping the symmetry intact.

The calculated Fe-W interlayer distances and magnetic moments for both the Fe and W atoms are listed in Tables I and II, respectively. The equilibrium Fe-W interlayer distance is 1.97 Å for 1 ML Fe/W(110), a relaxation of  $\sim 13\%$  from the bulk W-W(110) interlayer distance. This value is in reasonable agreement with the earlier low-energy electron diffraction (LEED) experiment result of 13% relaxation<sup>5</sup> and the recent scattering x-ray diffraction (SXRD) result of 8% relaxation.<sup>24</sup> A much smaller Fe-W interlayer spacing of 1.88 Å was determined by earlier FP-LAPW calculations,<sup>2</sup> a relaxation of 16%. On the other hand, our theoretical Fe-W interlayer distance is only 1.25 Å in 1 ML Fe/W(100) for the same in-plane lattice spacing of 3.205 Å as in Fe/W(110), a relaxation of  $\sim 22\%$  compared to the corresponding W-W

TABLE I. Theoretical atomic structures for 1 ML Fe/W(110) and Fe/W(100).

	$d(\text{Fe}-\text{W}_1)$ (Å)	$d(\text{W}_1-\text{W}_2)$ (Å)	$d(\text{W}_2-\text{W}_3)$ (Å)
1 ML Fe/W(110) ( $a=3.205$ Å)	1.97	2.26	2.25
1 ML Fe/W(100) ( $a=3.205$ Å)	1.25	1.61	1.60
1 ML Fe/W(100) ( $a=3.165$ Å)	1.28	1.64	1.61
1 ML Fe/W(100) ( $a=3.123$ Å)	1.30	1.66	1.63

TABLE II. Theoretical magnetic moments for 1 ML Fe/W(110) and Fe/W (100).

	$\mu_B$ (Fe)	$\mu_B$ (W <sub>1</sub> )	$\mu_B$ (W <sub>2</sub> )	$\mu_B$ (W <sub>3</sub> )
1 ML Fe/W(110) ( $a = 3.205 \text{ \AA}$ )	2.56	-0.085	-0.000053	-0.00027
1 ML Fe/W(100) ( $a = 3.205 \text{ \AA}$ )	2.09	-0.25	0.090	-0.076
1 ML Fe/W(100) ( $a = 3.165 \text{ \AA}$ )	2.05	-0.24	0.094	-0.068
1 ML Fe/W(100) ( $a = 3.123 \text{ \AA}$ )	1.96	-0.23	0.082	-0.065

bulk interlayer distance. Earlier calculations by Wu and Freeman<sup>7</sup> show a Fe-W interlayer spacing of only  $1.07 \text{ \AA}$ , again much smaller than our current result. Their systematically smaller Fe-W interlayer distances is probably due to the treatment of W  $5p$  orbital as a core state, instead of as a semicore state adopted in our current calculations. Varying the in-plane lattice parameter for the 1 ML Fe/W(100) system only induces small changes in the interlayer distances as seen from Table I. The symmetry effect is more dramatic than shear lattice parameter variation.

Figures 3(a) and 3(b) show the minority-spin  $3d$  partial density-of-states ( $d$ -PDOS) for the Fe overlayer on W(100) and W(110) substrates, respectively. It is seen that the splittings of  $3d$  minority-spin bands are quite different for the two systems. For monolayer Fe grown on W(100) substrate, three major peaks could be identified, while for monolayer Fe grown on W(110) substrate, only two main peaks are seen. However, the Fe majority-spin  $3d$  band is almost completely filled.<sup>19</sup> The band is narrower compared to the minority spin  $3d$  band. Further there is no crystal-field splitting. This difference between the Fe minority-spin and majority-spin  $3d$  band is due to the different locations of these two bands. The majority-spin band is lower in energy and closer to the nuclei, therefore the influence of the neighboring atoms is much smaller. The minority-spin band, on the other hand, is higher in energy and further away from the nuclei, therefore crystal-field effect is much stronger.

Table II shows the magnetic moments for the Fe overlayer and the W substrate atoms. The magnetic moments for Fe are  $2.56\mu_B$  and  $2.09\mu_B$  for 1 ML Fe grown on W(110) and W(100) substrates, respectively. It appears that the magnetic moment of Fe is enhanced by 16% in 1 ML Fe/W(110) com-

pared to the bulk bcc Fe value of  $2.2\mu_B$  in agreement with previous experimental results.<sup>3,8</sup> However, a reduction of 5% is observed for the 1 ML Fe grown on W(100) substrate compared to the bulk Fe bcc value. Varying the lattice parameter in 1 ML Fe/W(100) changes very little of the magnetic moment. The more striking differences between the two systems come from the induced moments on the neighboring W layers. The interfacial W atom in (110) film acquires a moment of  $0.085\mu_B$  and is antiferromagnetically coupled to the neighboring Fe atoms. The magnetic moments for the interfacial W atoms in the (100) films are around  $0.25\mu_B$ , much larger compared to the ones in the (110) film. Recent experimental data<sup>37</sup> also demonstrate an induced interfacial W moment of  $\sim 0.2\mu_B$  for Fe/W(100) in good agreement with our current calculations. The inner W atoms have very small induced moments in the (110) film, while the induced moments for W persist for the inner layers in the (100) films. The second and third layer W atoms have moments of  $\sim 0.09\mu_B$  and  $\sim 0.07\mu_B$ , respectively, in the (100) oriented films. Each W layer in the (100) films is antiferromagnetically coupled to the neighboring layers, while all the W layers are ferromagnetically coupled to each other in the (110) film. These differences can be explained using crystal-field theory below for the adsorbed Fe atoms on W substrates.

As stated earlier, Fe/W(110) and Fe/W(100) have different symmetries with a  $C_{2v}$  point-group symmetry in the (110) film and  $C_{4v}$  symmetry in the (100) film as shown in Fig. 1. Further, the nearest-neighbor bond distances are also quite different. Fe has four equivalent nearest bonds  $a$  in the (100) plane while Fe has four bonds at a shorter distance of  $0.866a$  in the (110) plane. However, the Fe-W interlayer distance is much shorter for the (100) film than that of (110) film as described earlier. According to crystal-field theory, the otherwise degenerate Fe  $3d$  orbitals will be split according to the symmetries of the  $d$  orbitals, and to the geometric positioning of the nearest-neighbor atoms. The splitting will also depend on the strength of crystal field specific to each individual species. As stated earlier, Fig. 2 illustrates the splitting of Fe  $3d$  orbitals in two different crystal symmetries with and without the W substrate. The  $d$ -orbital symmetry also affects the nature of bonding with W substrate differently for the (100) and (110) crystallographic orientations. In the case of Fe/W(100),  $d_{xz}$  and  $d_{yz}$  orbitals are equivalent. However, the  $d_{xz}$  and  $d_{yz}$  orbitals are no longer degenerate in Fe/W(110) due to the reduced symmetry in Fe-Fe bonding.-

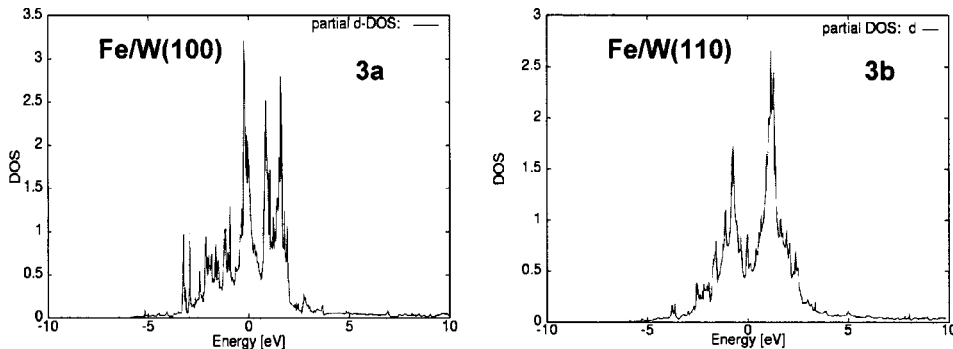


FIG. 3. Minority-spin  $3d$  partial density of states ( $d$ -PDOS) for Fe in 1 ML Fe/W(100) (a) and 1 ML Fe/W(110) (b).



TABLE III. The contribution of each orbital to the magnetic moment (spin-up–spin-down) inside the muffin-tin sphere ( $R=1.27 \text{ \AA}$ ) on each atom for 1 ML Fe/5 ML W(100).

Spin ( $\downarrow\uparrow$ )	$\mu_B$	$s$	$p$	$d_{\text{tot}}$	$d_{z^2}$	$dx^2y^2$	$d_{xy}$	$d_{xz}$	$d_{yz}$
W(S-3)	-0.076	-0.003	-0.003	-0.07	-0.012	0.05	-0.04	-0.022	-0.001
W(S-2)	0.091	0.002	-0.005	0.094	-0.018	-0.009	0.021	0.066	0.034
W(S-1)	-0.147	-0.01	-0.012	-0.125	-0.025	-0.04	-0.031	-0.064	-0.064
Fe(S)	2.096	0.033	0.004	2.059	0.628	0.521	0.189	0.391	0.331

The Fe-W bonds are formed through the interactions between the Fe  $4s$ ,  $4p_z$ ,  $3d_{z^2}$ ,  $3d_{xz}$ ,  $3d_{yz}$  orbitals and the W  $6s$ ,  $6p_z$ ,  $5d_{z^2}$ ,  $5d_{xz}$ ,  $5d_{yz}$  orbitals. The interaction between the interfacial Fe and W layers could be considered electronically favored in the Fe/W(100) system and electronically not favored in the Fe/W(110) system due to the  $C_{4v}$  symmetry of the former,  $C_{2v}$  symmetry of the latter, and the symmetries of the  $d_{xz}$  and  $d_{yz}$  orbitals. Both  $d_{xz}$  and  $d_{yz}$  orbitals are bonding orbitals in Fe/W(100) system, while  $d_{xz}$  orbital becomes strongly antibonding in Fe/W(110) system. This in turn leads to a stronger Fe-W bonding in Fe/W(100) films compared to the one in Fe/W(110). The observed smaller Fe-W interlayer distance of  $1.25 \text{ \AA}$  in the Fe/W(100) film compared to the distance of  $1.97 \text{ \AA}$  in Fe/W(110) film is a direct reflection of the stronger Fe-W interaction in the (100) film. Further, the observed reduced Fe moment of  $\sim 2.0\mu_B$  and enhanced W moment of  $0.25\mu_B$  in Fe/W(100) is due to the stronger interaction between Fe and W atoms in the (100) symmetry. The enhanced Fe moment of  $2.56\mu_B$  and smaller interfacial W moment of  $0.1\mu_B$  are due to the relative weaker interaction between Fe and W atoms in the (110) film. Decreasing the in-plane lattice parameter from  $3.205$  to  $3.123 \text{ \AA}$  while keeping the same symmetry in Fe/W(100) changes the magnetic moment slightly from  $2.09\mu_B$  to  $1.96\mu_B$ . The differences observed between different crystallographic orientations are more dramatic.

The magnetic “dead layer” observed in the submonolayer Fe coverage on W(100) substrate<sup>6,21</sup> could be partially attributed to the reduced moments calculated here for Fe/W(100). However, there must be other mechanisms contributing to the complete suppression of magnetic signal. It is possible that the Curie temperature for the 1 ML Fe/W(100) system is much lower than the corresponding Curie temperature of  $282 \text{ K}$  for the 1 ML Fe/W(110). It is known that Curie temperature is very sensitive to the film thickness, the coordination number, the capping and substrate layer thickness, and the interatomic distance.<sup>4,39–42</sup> Since exchange coupling  $J$  decays as  $\sim 1/R^3$ ,<sup>43</sup> in which  $R$  is the interatomic distance, the Curie temperature will be dependent upon the crystallographic orientation of the thin film as demonstrated in Ref. 42. Since Curie temperature is proportional to exchange coupling  $J$ , the Curie temperature for 1 ML Fe/W(100) will be around  $100 \text{ K}$  if only nearest-neighbor coordination and distance are considered. This temperature is below the previous experimental temperature conducted.<sup>6,21</sup> The lower magnetic moment for the monolayer Fe on W(100) substrate will reduce the Curie temperature even further compared to the corresponding W(110) substrate case.<sup>42</sup> In the submonolayer

regime, the Curie temperature is expected to be even lower due to the lower coordination number at such coverage compared to the complete monolayer coverage. All in all, our theoretical calculation does not find a magnetically dead monolayer Fe on W(100). However, it is possible that the Curie temperature of this system is far below the 1 ML Fe/W(110) case and below the experimental temperature conducted.

Interlayer exchange coupling is also affected quite strongly by the Fe-W interaction and by the symmetry of the system. One indirect measure of interlayer exchange coupling strength is via the induced moments on the W substrate atoms. As stated previously, the interfacial W atom has an induced moment of  $\sim 0.2\mu_B$  in (100) oriented film compared to  $\sim 0.085\mu_B$  in (110) oriented film. Further, the inner W moments vanish very quickly in (110) films, while they are quite substantial in (100) films. The observed strong exchange coupling in (100) oriented multilayers is directly related to the stronger interaction between the layers in (100) oriented films. The difficulty in observing the short GMR oscillation periods in (110) oriented films is probably related to weak interlayer interaction in (110) films. It is relatively easier to understand qualitatively how roughness affects the interlayer exchange coupling using the above argument. Basically roughness weakens the crystal-field effect due to the reduction of coordination number in the rougher films. Further roughness and disorder at interfaces lead to the incommensurate interlayer interaction in the films and therefore the weak coupling between the layers.

As shown in Tables I and II, the interlayer distance influences the magnetic coupling between the W layers. For the shorter interlayer distance in Fe/W(100) films, the induced moments on each W layer are antiferromagnetically coupled to each other. The larger interlayer distance in Fe/W(110) films causes the W layers to be ferromagnetically coupled to each other even though the induced moments are very small.

Tables III and IV list the contributions to the total magnetic moment by each individual orbital for 1 ML Fe/W(100) and 1 ML Fe/W(110), respectively. It can be seen that only  $d$  orbitals make substantial contribution to the total local magnetic moment. Moreover, the relatively high-lying antibonding orbitals make the most significant contribution to the magnetic moment. In Fe/W(100), these are the  $d_{z^2}$  and  $dx^2y^2$  orbitals that make the largest contributions to the Fe magnetic moment. In Fe/W(110), these are the  $d_{z^2}$ ,  $d_{xz}$  and  $dx^2y^2$  orbitals.

The reason for violating Hund’s third rule due to crystal-

TABLE IV. The contribution of each orbital to the magnetic moment (spin-up–spin-down) inside the muffin-tin sphere ( $R=1.217 \text{ \AA}$ ) on each atom for 1 ML Fe/5 ML W(110).

Spin ( $\downarrow\uparrow$ )	$\mu_B$	$s$	$p$	$d_{\text{tot}}$	$dz^2$	$dx^2y^2$	$dxy$	$dxz$	$dyz$
W( $S$ -3)	-0.001	-0.001	-0.003	0.003	-0.002	0.001	0.002	0.003	0.001
W( $S$ -2)	-0.001	0.000	-0.002	0.001	0.006	-0.001	-0.008	0.005	-0.002
W( $S$ -1)	-0.088	-0.003	-0.012	-0.073	-0.022	0.017	0.001	-0.047	-0.021
Fe( $S$ )	2.562	0.020	-0.005	2.547	0.585	0.608	0.411	0.665	0.279

field effect is also obvious from Fig. 2. If the electron exchange energy is larger than the energy splitting between the bonding and antibonding orbitals, the system will lower its energy by keeping both the bonding and antibonding orbitals partially occupied and their electron spins aligned parallel to each other. However, if the crystal-field splitting is larger than the electron exchange energy, the system will gain by energy if the electrons spins are paired and electrons occupy the bonding orbitals. It is apparent that Hund's third rule will only be valid for lighter transition metals since the crystal-field effects for these elements are small. In the case of W, there is a large crystal-field splitting in W due to the stronger interatomic interaction of the  $5d$  orbitals. Since the average exchange splitting is around 1.6 eV in Fe and much smaller for W, and there are  $5d$  orbitals spread over the  $d$  band of 10 eV for W, it is easier to see that exchange splitting is smaller than the average energy difference between the  $d$  orbitals. Thus Hund's third rule is no longer valid for the W systems. For Fe/W(100) and Fe/W(110), there is another possible reason for the violation of Hund's third rule for the interfacial W layers due to the interlayer spin-orbit interaction with the Fe moments as pointed out by Wilhelm *et al.*<sup>37</sup> But generally Hund's third rule will not be applicable when there is a large crystal field present.

#### IV. SUMMARY

It is shown that symmetry and crystal-field effect are important factors in determining the equilibrium atomic and electronic structures in ultrathin Fe/W(110) and Fe/W(100) magnetic films. The crystal-field energy splitting of the outer  $d$  orbitals and their relative positions are strongly symmetry dependent. As a result, the magnetic interactions including exchange coupling and magnetic moments are strongly affected by the crystal-field splitting and therefore by the symmetry of the thin films. Symmetry also mediates the interactions between the Fe overlayer and W substrates. In Fe/W(100), a stronger interaction between Fe and W is observed, while a weaker interaction between the layers is found in Fe/W(110) films. The lack of experimental evidence on the short oscillation periods in (110) oriented GMR films could also be attributed partly to the weak interlayer interaction in the (110) films. The violation of Hund's third rule in the interfacial W layers is probably due to the strong crystal-field splitting in W  $5d$  orbitals.

#### ACKNOWLEDGMENTS

The authors would like to thank Professor J. Kirschner for his continued support and Dr. Sander for the critical reading of the manuscript.

<sup>1</sup>G. Waller and U. Gradmann, Phys. Rev. B **26**, 6330 (1982).

<sup>2</sup>S. Hong, A. Freeman, and C. Fu, Phys. Rev. B **38**, 12 156 (1988).

<sup>3</sup>H. J. Elmers, G. Liu, and U. Gradmann, Phys. Rev. Lett. **63**, 566 (1989).

<sup>4</sup>W. Weber, D. Kerkmann, D. Pescia, D. A. Wesner, and G. Güntherodt, Phys. Rev. Lett. **65**, 2058 (1990).

<sup>5</sup>M. Albrecht, U. Gradmann, T. Reinert, and L. Fritsche, Solid State Commun. **78**, 671 (1991).

<sup>6</sup>G. A. Mulhollan, R. L. Fink, J. L. Erskine, and G. K. Walters, Phys. Rev. B **43**, 13 645 (1991).

<sup>7</sup>R. Wu and A. J. Freeman, Phys. Rev. B **45**, 7532 (1992).

<sup>8</sup>U. Gradmann, in *Handbook of Magnetic Materials*, edited by K. H. J. Buschow (Elsevier Science B.V., North-Holland, 1993), Vol. 7, Chap. 1, pp. 1–96.

<sup>9</sup>H. Elmers, J. Hauschild, H. Höche, U. Gradmann, H. Bethge, D. Heuer, and U. Köhler, Phys. Rev. Lett. **73**, 898 (1994).

<sup>10</sup>H. Elmers, J. Hauschild, H. Fritzsche, G. Liu, U. Gradmann, and U. Köhler, Phys. Rev. Lett. **75**, 2031 (1995).

<sup>11</sup>M. Plihal, D. L. Mills, H. J. Elmers, and U. Gradmann, Phys. Rev. B **51**, 8193 (1995).

<sup>12</sup>D. Sander, R. Skomski, C. Schmidthals, A. Enders, and J. Kirschner, Phys. Rev. Lett. **77**, 2566 (1996).

<sup>13</sup>H. Tang, M. Plihal, and D. L. Mills, Phys. Rev. B **54**, 14 172 (1996).

<sup>14</sup>N. Weber, K. Wagner, H. J. Elmers, J. Hauschild, and U. Gradmann, Phys. Rev. B **55**, 14 121 (1997).

<sup>15</sup>E. Tober, R. Ynzunza, F. Palomares, Z. Wang, Z. Hussain, M. van Hove, and C. Fadley, Phys. Rev. Lett. **79**, 2085 (1997).

<sup>16</sup>J. Hauschild, U. Gradmann, and H. J. Elmers, Appl. Phys. Lett. **72**, 3211 (1998); J. Hauschild, H. J. Elmers, and U. Gradmann, Phys. Rev. B **57**, R677 (1998).

<sup>17</sup>D. Sander, A. Enders, C. Schmidthals, D. Reuter, and J. Kirschner, Surf. Sci. **402–404**, 351 (1998).

<sup>18</sup>D. Sander, Rep. Prog. Phys. **62**, 809 (1999).

<sup>19</sup>X. Qian and W. Hübner, Phys. Rev. B **60**, 16 192 (1999).

<sup>20</sup>D. Sander, A. Enders, and J. Kirschner, Europhys. Lett. **45**, 208 (1999).

- <sup>21</sup>W. Wulfhekel, W. F. Zavaliche, F. Porrati, H. P. Oepen, and J. Kirschner, *Europhys. Lett.* **49**, 651 (2000).
- <sup>22</sup>I. Galanakis, M. Alouani, and H. Dreyssé, *Phys. Rev. B* **62**, 3923 (2000).
- <sup>23</sup>X. Qian and W. Hübner, *Phys. Rev. B* **64**, 092402 (2001).
- <sup>24</sup>H. L. Meyerheim, D. Sander, R. Popescu, and J. Kirschner, *Phys. Rev. B* **64**, 045414 (2001).
- <sup>25</sup>P. Grünberg, R. Schreiber, Y. Pang, M. B. Brodsky, and H. Sower, *Phys. Rev. Lett.* **57**, 2442 (1986); S. S. P. Parkin, N. More, and K. P. Roche, *ibid.* **64**, 2304 (1990).
- <sup>26</sup>Y. Yafet, *Phys. Rev. B* **36**, 3948 (1987); C. Chappert and J. P. Renard, *Europhys. Lett.* **15**, 553 (1991); P. Bruno and C. Chappert, *Phys. Rev. Lett.* **67**, 1602 (1991); **67**, 2592(E) (1991); P. Bruno and C. Chappert, *Phys. Rev. B* **46**, 261 (1992); R. Coehoorn, *ibid.* **44**, 9331 (1991).
- <sup>27</sup>D. E. Edwards, J. Mathon, R. B. Muniz, and M. S. Phan, *Phys. Rev. Lett.* **67**, 493 (1991); J. Mathon, M. Villeret, and D. M. Edwards, *J. Phys.: Condens. Matter* **4**, 9873 (1992).
- <sup>28</sup>P. Bruno, *Magnetism: Molecules to Materials III Nanosized Magnetic Materials*, edited by Joel S. Miller and Marc Drillon (WILEY-VCH, Weinheim, 2002), pp. 329–353.
- <sup>29</sup>L. Nordström, P. Lang, R. Zeller, and P. H. Dederichs, *Phys. Rev. B* **50**, 13 058 (1994).
- <sup>30</sup>N. Lathiotakis, B. L. Györfy, and B. Újfalussy, *Phys. Rev. B* **61**, 6854 (2000).
- <sup>31</sup>J. E. Hirsch, *Phys. Rev. B* **56**, 11 022 (1997).
- <sup>32</sup>T. Momoi and K. Kubo, *Phys. Rev. B* **58**, R567 (1998).
- <sup>33</sup>C. D. Batista, J. Bonča, and J. E. Gubernatis, *Phys. Rev. Lett.* **88**, 187203 (2002).
- <sup>34</sup>E. C. Stoner, *Proc. R. Soc. London, Ser. A* **154**, 656 (1936).
- <sup>35</sup>A. Hjelm, O. Eriksson, and B. Johansson, *Phys. Rev. Lett.* **71**, 1459 (1993).
- <sup>36</sup>I. Galanakis, P. M. Oppeneer, P. Ravindran, L. Nordström, P. James, M. Alouani, H. Dreyssé, and O. Eriksson, *Phys. Rev. B* **63**, 172405 (2001).
- <sup>37</sup>F. Wilhelm, P. Pouloupoulos, H. Wende, A. Scherz, and K. Baberschke, *Phys. Rev. Lett.* **87**, 207202 (2001).
- <sup>38</sup>P. Blaha, K. Schwarz, and J. Luitz, “WIEN97, A full potential linearized augmented plane wave package for calculating crystal properties,” Karlheinz Schwarz, Tech. Univ. Wien, Vienna, 1999.
- <sup>39</sup>C. M. Schneider, P. Bressler, P. Schuster, and J. Kirschner, *Phys. Rev. Lett.* **64**, 1059 (1990).
- <sup>40</sup>R. Vollmer, S. van Dijken, M. Schleberger, and J. Kirschner, *Phys. Rev. B* **61**, 1303 (2000).
- <sup>41</sup>M. Pajda, J. Kudrnovský, I. Turek, V. Drchal, and P. Bruno, *Phys. Rev. Lett.* **85**, 5424 (2000).
- <sup>42</sup>R. Zhang and R. F. Willis, *Phys. Rev. Lett.* **86**, 2665 (2001).
- <sup>43</sup>M. Pajda, J. Kudrnovský, I. Turek, V. Drchal, and P. Bruno, *Phys. Rev. B* **64**, 174402 (2001).